JCAMECH

Vol. 47, No. 1, June 2016, pp 79-87
DOI: 10.22059/jcamech.2016.59257

Design and implementation of an unmanned aerial vehicle for inspection of electricity distribution networks

Mohammad Hosein Salimi, Majid Roshanfar*

Faculty of Mechanical Engineering, K.N. Toosi University of Technology, Tehran, Iran

Received: 15 Mar. 2016 , Accepted: 27 May 2016

Abstract

One of the most crucial elements of each country is electricity distribution networks (EDN). Awareness of accidents in EDN could be very important in the conservation and utilization of them. The accurate and periodic inspections can provide a good service to subscribers. The goal of this project is to fabricate a quad rotor, which can do an accurate and a periodic inspection. The design and implementation procedure are explained. The mechanical parts are designed by SolidWorks software then the structure of robot is fabricated with AL8080 by machining and milling. Then the dynamic model of the robot is generated and based on it the controller is designed. The two PID controller are proposed and simulated with MATLAB Simulink.

Keywords:

Electricity distribution network, Inspection, UAV, Design and implementation

1. Introduction

The electric distribution network (EDN) consists of pylons and cables that deliver electric power from power plants to users. Nowadays, EDNs are seen in all parts of the world. Designing, manufacturing, installing and maintaining of EDNs are very important and complicate. Regular inspections and periodic maintenance are big challenges. EDNs are vast networks, so inspection is costly and time-consuming. In the past decades, the procedure of maintenance and repairing gradually are changed. The most important methods are used in Iran is as follows:

- Aerial inspection [2] (preventive): In this method according to the extent and importance of the network and condition of geographical area, helicopters are used to inspect. This method is a quick and a global inspection.
- Tower inspection [2] (emergency): This method is usually used after failures that occur in EDNs. Inspectors repair damaged pylons or towers locally. This method takes more time and usually has life threatening. Therefore, inspection and climbing for technicians has dangers and costs.

According to the type of environment and level transition, there are power pylons with different heights. The height of high voltage pylons usually is 50 to 100 meters [1]. There are four major categories of transmission towers [1]: suspension, terminal, tension, and transposition. Some transmission towers

* Corresponding Author. Tel.: +98 9363925762. Email Address: Majidroshanfar@ut.ac.ir

combine these basic functions.

Towers may be self-supporting and capable of resisting all forces due to conductor loads, unbalanced conductors, wind and ice in any direction. Such towers often have approximately square bases and usually four points of contact with the ground. Figure 1 shows structures of the suspension pylons.

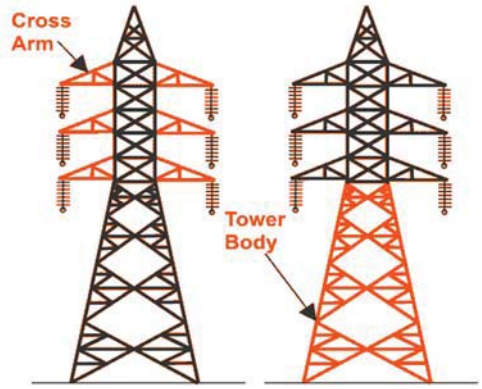

Figure 1- Suspension Towers

2. Robots and inspection

Today, robots are used to do tasks that are hard or impossible for humans. Accuracy and speed are advantages of robots in a mission [5]. The Unmanned aerial vehicle (UAV) is a branch of robots that can fly and collect information and send it to their land base. UAVs reach easily to out of access goals, so we can use these robots for inspection of electricity pylons [6]. In addition, because these robots are unmanned and remotely controlled, there is not any danger for technicians.

These robots carry sensors and other detection equipment's [4]. If a camera is mounted on the robot, it can collect and send images to the ground station [9]. Figure 3 shows two captured photos of a pylon

Figure 2- The UAV is inspecting pylons

Figure 3- Two captured photo from cables and towers

3. UAVs

There are many types of UAVs based on the platforms. One of the most important types is the quad rotor. A Quad copter, also called a quad rotor helicopter or quad rotor, is a multirotor helicopter that is lifted and propelled by four rotors [1]. Quad copters are classified as rotorcraft, as opposed to fixed-wing aircraft, because their lift is generated by a set of rotors (vertically oriented propellers) [5&7]. Quad copters generally use two pairs identical fixed pitched propellers; two clockwise (CW) and two counter-clockwise (CCW) [3]. This configuration allows quad rotors to move easily in all directions and have excellent maneuverability. There are several advantages of quadrotors over similar scaled helicopters. First, standard quadrotors are mechanically less complex than helicopters due to the absence of the sophisticated rotor hub. This greatly simplifies the design and maintenance of the quadrotor. Second, the use of four small-diameter rotors (usually) allows quadrotors to possess less kinetic energy during flight as compared to helicopters. The thrust is controlled by modifying the rotational velocity of the rotors. As a rotor spins around its axis, an opposing torque (due to propeller blades aerodynamic drag) is generated around the rotor axis. In hovering or in vertical climb/descent, all rotors spin at the same speed. Due to the counter rotating nature of the two rotor pairs and the aforementioned symmetric property, the net torque on the quad rotor is zero; thereby no yaw motion is generated. Roll and pitch control can be achieved by increasing the speed of one rotor and decreasing that of the diagonally opposite rotor. The yaw control is achieved by the difference between the torques between a pair of opposite rotors and the remaining pair.

4. Mechanical parts

Quad rotors mechanical implementation process involves the following steps:

Basic design ⟹ Mechanical calculations ⟹ Computer-aided design with Solid Works software

Implementation ⟹ Test

The frame also must have a low weight, and good mechanical strength. In addition, the most important challenge to design structure is the center of mass balancing. Quad rotors frame shape is like a plus sign[3]. Four arms are joined to the central disk. The central disc consists of two parts, which are as bearing for each arm. The mechanical stress reduction of the central disk and the vibration reduction are the advantage of this design. After the calculation of the mechanical design, the detail design of the robot is drawn by software Solid Works. The 6th series of aluminum is selected for fabrication [5]. This aluminum has a good mechanical strength and low weight [6]. (Table 8)

Table 1 Alluminium properties

Series	Additive	Tensile strength
1xxx	Min 99% aluminum	10-27 ksi
2xxx	copper	27-62 ksi
3xxx	Manganese	16-41 ksi
4xxx	Silicon	25-55 ksi
5xxx	Magnesium	18-51 ksi
6xxx	Magnesium and silicon	18-58 ksi
7xxx	Zinc	32-88 ksi

After selecting material, next step is implementation parts of the robot. The parts are produced by machining, grinding, polishing and drilling operations. Finally, the parts were assembled together according to the technical plan. (Figure 4-7)

Figure 4- Primery disk

Figure 5- Final disk that was product with machining

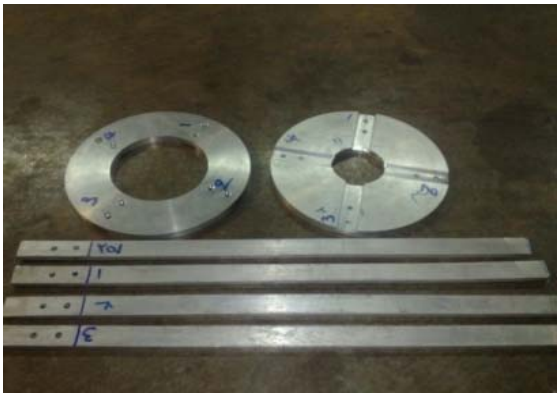

Figure 6- Part of frame before assembling

Figure 7- Assembled frame

5. Electronic parts

In this step, we tried to design a copilot to control the robot. A copilot should stabilize the robot, send and receive data [2]. A copilot consists of several sensors such as accelerometer, gyroscope andmagnetometer, one or more processors and some peripherals [7]. The copilot consists of four units:

- Central processor unit

- Sensors
- Actuators driver unit
- Data receiver and transmitter

5.1. *Central processor unit*

This part is the main parts of the copilot system and consists of a microprocessor. The task of the microprocessor is receiving and decoding sensor's information, processing these data, and controlling the actuators [2]. This robot has a main processor and several sub processors, each of them has specific task. Sub processors, receive the information from the ground base station and sensors, then decode them and send decoded data to the main processor. The main processor, process received data's. Regard to the received orders by grand station, the main processor send command to the driver units. For real time control, the main processor must be high-speed. The Atmega 328 is selected for this purpose. This processor has high processing speed, tiny dimension and it can control several slave processors real-timely. Also, The Atmega 32 is selected as sub processor. (Figure 8)

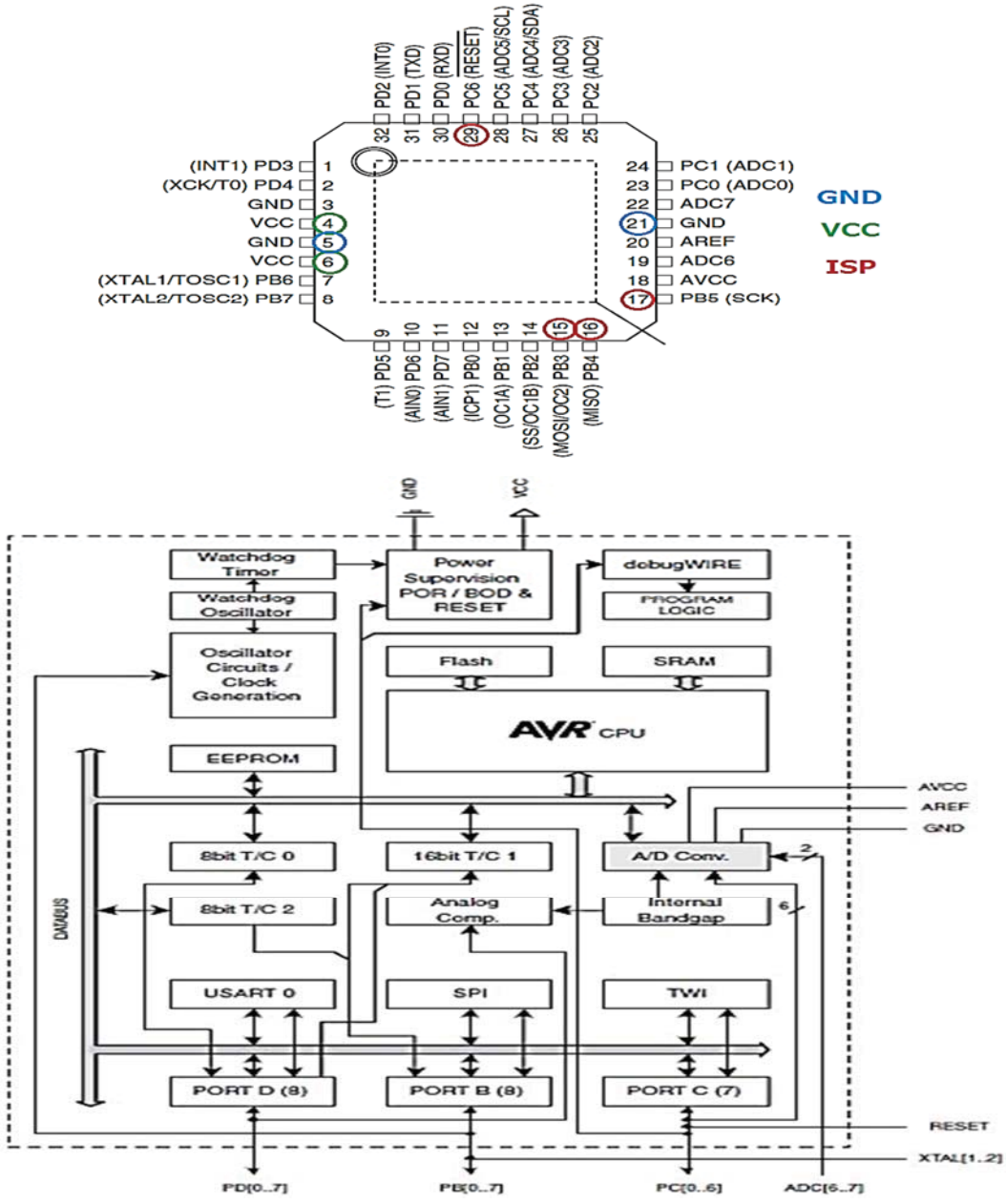

Figure 8- Schematic of Atmega 328

5.2. *Sensor*

The tasks of Sensors in the robot are sensing and collecting necessary information. Because Quad rotors inherently are very unstable, sensors should sense the stability and statues of the system. The main sensors used in the UAV are the gyroscope and the accelerometer. The gyro sensor measures the angular velocity of the UAV in three axes. Accelerometer sensor can measure the linear acceleration [3]. Due to applications of UAV's, various sensors, such as camera sensors, humidity gauges, pressure sensors, distance meter, global positioning system, can be mounted on the robot [4].

5.3. *Actuator*

In flying robots, motors and propellers play main role in taking off mode. Therefore, they should have low weight and also produce enough thrust. In the robot, we have used brushless motors as thruster. Brushless motors like the other motors need to a driver. This driver unit also known as the speed control drivers. For driving the motor, the CPU should send pulses to the drivers. The frequency of the pulses is between 50 to 100 Hz and the pulse width is between 1 to 2 seconds. The increasing the pulse width, the increasing motors speed [2].

5.4. *Communication unit*

The communication unit sends and receives commands. A good connection should be stable, safe and has sufficient bandwidth. Using radio waves with appropriate wavelength is one of the most common ways to transmit information**.** A pair of commercially radio receivers and transmitters is used in the robot. Maximum range of transmission is about 3km and its frequency is 2.4 GHz, as well has 4 separate channels to send commands.

6. Control

The control type of the robot is semi-automatic control in this project. The necessary commends are sent to the robot by radio transmitter and ground station,. According to the conditions and received commends, CPU controls motors. A flying robot in space has six degree of freedom, so it is very unstable. As well as, other factors such as non-balanced frame and non-identical motors increase instability of the system [1]. A closed loop control systems, such as *PID* and FUZZY is appropriate to control [3]. The *PID* controller system is simple to implement and is not complicated. This control system collects proportional, integral and derivative error and compare these errors, finally send proper commends to motors.

7. Dynamic modeling

Quad rotors have four rotors with fixed pitch, in other word have four inputs. In Quad rotors the motor 1 and the motor 3, clockwise rotate and the motor 2 and the motor 4 rotate counterclockwise [9]. Quad rotors have 6 degrees of freedom that is determined in 12 terms. Desire position and vector control are as follows:

$$X = [\phi \quad \dot{\phi} \quad \theta \quad \dot{\theta} \quad \Psi \quad \dot{\Psi} \quad x \quad \dot{x} \quad y \quad \dot{y} \quad z \quad \dot{z}] \tag{1}$$

$$U = [u_1 \quad u_2 \quad u_3 \quad u_4]^T \tag{2}$$

u_i's are the motor's inputs. Six terms of the twelve's, relate to the rotation of the system. These terms include Euler angles and the angular velocity in the coordinate system. The other six terms, include position and linear velocity of mass center. By using the lagrangian and general form of the motion equations:

$$L = T_k - V \tag{3}$$

$$F = \frac{d}{dt}\left(\frac{\partial L}{\partial \dot{q}}\right) - \frac{\partial L}{\partial q} \tag{4}$$

Here L is lagrangian, T_k is kinetic energy and V is the potential energy. The vector q is a general vector and defined as follows:

$$q = [x \quad y \quad z \quad \phi \quad \theta \quad \Psi]^T \tag{5}$$

The vector F includes action force,F_E, and action momentum T.

$$F = (F_E, T) \tag{6}$$

For linear transition in Lagrange equations:

$$F_E = \frac{d}{dt}\left(\frac{\partial L}{\partial \dot{\xi}}\right) - \frac{\partial L}{\partial \xi} \tag{7}$$

Where general coordinates are:

$$\xi = [x \quad y \quad z]^T \tag{8}$$

The resultant forces vector can be written as product of angles matrix and motor thrust forces:

$$F_E = \begin{bmatrix} \sin\theta \\ -\sin\phi\ \cos\theta \\ \cos\phi\ \cos\theta \end{bmatrix} . f_g \tag{9}$$

Which:

$$f_g = F_1 + F_2 + F_3 + F_4 \tag{10}$$

The produced force by a motor has proportional relationship to square of rotational velocity. So we can write:

$$F_i = b\Omega_i^2 \tag{11}$$

The term Ω_i is equal to rotational velocity of motor and b is equal to thrust factor. Lagrange equation for rotational motion is:

$$T = \frac{d}{dt}\left(\frac{\partial L}{\partial \dot{\eta}}\right) - \frac{\partial L}{\partial \eta} \quad (12)$$

In the equation12:

$$\eta = [\phi \quad \theta \quad \Psi]^T \quad (13)$$

Which is also known as the Euler angles. Also:

$$T = [T_\phi \quad T_\theta \quad T_\Psi]^T \quad (14)$$

$$T_\phi = bl\,(\Omega_4^2 - \Omega_2^2) - J_r\dot{\theta}\,(\Omega_1 + \Omega_3 - \Omega_2 - \Omega_4) \quad (15)$$

$$T_\theta = bl\,(\Omega_3^2 - \Omega_1^2) - J_r\dot{\theta}\,(\Omega_1 + \Omega_3 - \Omega_2 - \Omega_4) \quad (16)$$

$$T_\Psi = d\;(\Omega_1^2 + \Omega_3^2 - \Omega_2^2 - \Omega_4^2) \quad (17)$$

The parameter l is equal to the distance between the blade and the center of mass, J_r is inertia of the rotor and d is the drag coefficient. Finally, the dynamic model of the quad rotor in x, y, z direction and roll, pitch, yaw motion like as following:

$$\ddot{\theta} = \frac{1}{I_{xx}}\left(-\dot{\phi}^2(I_{xx} - I_{zz})\,s(\theta)\,c(\theta) - \dot{\phi}\dot{\Psi}I_{zz}\,c(\theta) + T_\theta\right) \quad (18)$$

$$\ddot{\phi} = \frac{1}{I_{yy}\left(1 + s^2(\theta)\right)}\left(-\ddot{\Psi}I_{zz}\,s(\theta) - \dot{\theta}\dot{\phi}\,c(\theta)\,s(\theta)\,(2I_{zz} - 2I_{yy}) - \dot{\theta}\dot{\Psi}\,I_{zz}\,c(\theta) + T_\phi\right) \quad (19)$$

$$\ddot{\Psi} = \frac{1}{I_{zz}}\left(-\ddot{\phi}I_{zz}s(\theta) + T_\Psi\right) \quad (20)$$

$$\ddot{x} = \frac{f_g}{m}\,s(\theta) \quad (21)$$

$$\ddot{y} = -\frac{f_g}{m}\,c(\theta)\,s(\phi) \quad (22)$$

$$\ddot{z} = \frac{f_g}{m}\,c(\theta)\,c(\phi) - g \quad (23)$$

In the above equations, the term s is sine and the term c is cosine.

8. Actuating system

The dynamic model of actuating system includes DC motors and blades. The model of motors is obtained from a first order differential low inductance equation, as follows:

$$J_r\frac{d\omega_m}{dt} = \frac{k_m}{R}u - \frac{k_m k_e}{R}\omega_m - \tau_1 \quad (24)$$

Where u is motors input, R is motors resistance, k_e is motors constant, ω_m is motors angular velocity, J_r is rotors inertia, k_m is torques constant and τ_1 is motors load. The relationship between angular velocity and thrust is as follows:

$$F_T = C_T\rho D^4.n_P^2 \quad (25)$$

Thrust factor C_T is one of the propeller parameters and related to the term λ linearly:

$$\lambda = \frac{V}{n_P D} \quad (26)$$

That V is speed of air, n_P is the rotational speed of the blade, the term D is diameter of the blade and ρ is the air density.

9. Controller design

External noises reduction and improved performance are the most important challenges in controller design. For this purpose, the PID controller can be used [10]. A PID controller continuously calculates an "error value" as the difference between a measured process variable and a desired set point. The controller attempts to minimize the error over time by adjustment of a control variable [4]:

$$u(t) = K_P e(t) + K_i\int_0^t e(\tau)\,d\tau + K_d\frac{de}{dt} \quad (27)$$

WhereK_P, K_i, and K_d, all non-negative, denote the coefficients for the proportional, integral, and derivative terms, respectively (sometimes denoted P, I, and D). In this model, P accounts for present values of the error, I accounts for past values of the error, and D accounts for predicted future values of the error, based on its current rate of change. The proportional, integral, and derivative terms are summed to calculate the output of the *PID* controller. Defining $u(t)$ as the controller output, the final form of the *PID* algorithm is:

$$u(t) = MV(t) = K_P e(t) + K_i\int_0^t e(\tau)\,d\tau + K_d\frac{d}{dt}e(t) \quad (28)$$

Where:

K_P: Proportional gain, a tuning parameter
K_i: Integral gain, a tuning parameter
K_d: Derivative gain, a tuning parameter
$u = P + I + D$
e: Error = $SP - PV$
t: Time or instantaneous time (the present)
τ: Variable of integration; takes on values from time 0 to the present t
$e(t) = e_d(t) - e_a(t)$ (29)

In equation29 the term e_d is desire condition, e_a is real condition (measured) and $e(t)$ is equal to the difference (error) between the two time constant that is back together.[8] Each proportional and integral and derivative controller has its own gain and through of these, desired features for the *PID* controllers are obtained. The controller can be defined as follows:

$$P = k_P e(t) \qquad I = k_i \int_o^t e(\tau)\, dt$$
$$D = K_d \frac{de}{dt} \tag{30}$$

These factor considers between 0.25 to 0.5. To design the control loop, double loop control can be used. There are two control loops in this controller that is one of them as known as the inner loop and the other is known as outer loop. In this controller, the outer loop inputs are Euler angle and calculations in this loop is absolute by measuring the angle of the axis of Quad rotor. Finding a flying object which acceleration implies to their main axis can be done practically difficult [2]. So the inner controller loop can be used. The loop finds angular velocity by gyroscope data and it finds angels by integration and comparison to main axes. But in practice, the integration has cumulative errors; an accelerometer with gyro can also be used. Accelerometer can sense the tilt angles absolutely through comparing to gravity [6].

10. Internal and external PID controller

In both internal and external loops, two types of PID controls can be considered. (Figure 9)

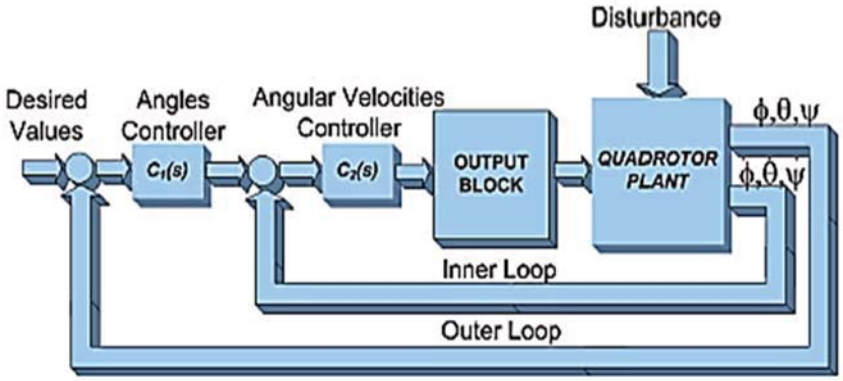

Figure 9- Control loop

In control theory, ideal *PID* controllers in parallel structure define in continuous period:

$$u(t) = K_P e(t) + K_i \int_0^t e(\tau)\, d\tau + K_d \frac{de(t)}{dt} \tag{31}$$

In equation 31 K_i is the integral gain, K_d is derivative gain and K_P is proportional gain. The main problem of conventional PID controller is their response to the input's changes product an impulse function on the controller. So to solve this problem, there is another control structure [16]. Actually, Type B controller is a combination of PI controller and D controller, which is written as PI-D. The equation is as follows [24]:

$$u(t) = K_P e(t) + K_i \int_0^t e(\tau)\, d\tau - K_d \frac{dy(t)}{dt} \tag{32}$$

The block diagrams of the equations are in figure 10 and figure 11:

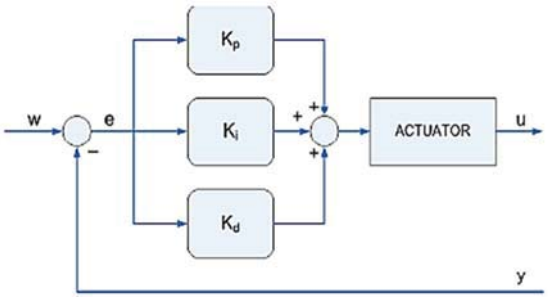

Figure 10- PID controller

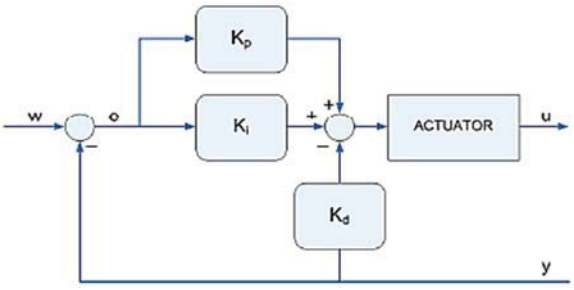

Figure 11- PI-D controller

11. Simulation

The simulation is used to evaluate the controller design and to find the best gains. The model is simulated by the MATLAB Simulink. According to the simulation, graphs of the results are plotted in figure 12 and 13. The quad rotor system is supplied by a step function. Looking at the step responses, it is clear that each control system has a different response for the same attitudes. However, it is possible to choose the most suitable technique based on the characteristics that are needed for the quad copter. On the other hand, a PID controller gives a faster response but not with robust gains as the PI-D controller. The classic PID theory implies in not developing a robust controller. In addition, the simulation results show that the PI-D controllers are able to stabilize the quad rotor helicopter robustly and move it to a desired position with a desired yaw angle.

12. Conclusion

In this paper, we propose a new paradigm of power line inspection by using cooperative UAVs. Then one of the most important flying robots, Quad rotors, was introduced and its principal was discussed. The details of UAV functionality and communication systems are introduced and discussed. Our practical experience shows that by this cooperative operation, the time taken for inspection can be greatly reduced and the efficiency can be improved tremendously. The feasibility and superiority of UAV inspection is demonstrated. The further work may include the optimization of UAV configuration in crew team.

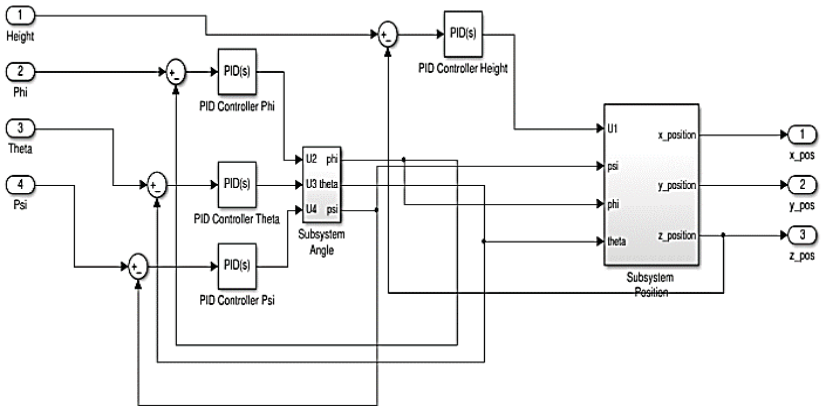

Figure 12- PID simulation with Simulink

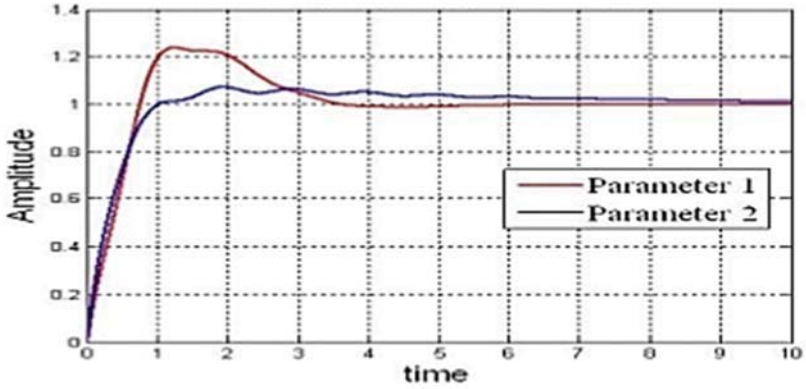

Figure 13- graph of the results, blue line(parameters2) is the PI-D and red line (parameter1) is the PID controller

13. References

[1] S. Mukhopadhyay, "PID equivalent of optimal regulator," Electronics Letters, vol. 14, no. 25, pp. 821–822, 1978.

[2] S. Bouabdallah, A. Noth, and R. Siegwart, “PID vs LQ control techniques applied to an indoor micro quadrotor,” in proceedings of IEEE International Conference on Intelligent Robots and Systems IROS, 2004, pp. 2451–2456.
[3] A. L. Salih, M. Moghavvemi, H. A. F. Mohamed, and K. S. Gaeid, “Flight PID controller design for a UAV quadrotor,” Scientific Research and Essays, vol. 5, pp. 3360–3367, 2010.
[4] T. Madani and A. Benallegue, “Backstepping control for a quadrotor helicopter,” Intelligent Robots and Systems, 2006 IEEE/RSJ International Conference on, pp. 3255–3260, 2006.
[5] G. V. Raffo, M. G. Ortega, and F. R. Rubio, “An integral predictive/ nonlinear H infinity control structure for a quadrotor helicopter,” Automatica, vol. 46, pp. 29–39, 2009.
[6] M. Jun, S. I. Roumeliotis, and G. S. Sukhatme, “State estimation of an autonomous helicopter using Kalman filtering,” in Intelligent Robotsand Systems, 1999, pp. 1346 – 1353.
[7] D. Jones, “Power line inspection - a UAV concept,” in Proc. *IEE Forum on: Autonomous Systems*, 2005 pp. 1-7.
[8] J. Katrasnik, F. Pernus, B. Likar, “A Survey of Mobile Robots for Distribution Power Line Inspection,” *IEEE Trans. on Power De-livery*, vol. 25, pp. 485-493, Jan 2010.
[9] J. Toth, and G.J. Adelana, "Smart view for a smart grid—Unmanned Aerial Vehicles for transmission lines,” in *Proc. IEEE Applied Robotics for the Power Industry*, Montreal, 2010, pp. 1-6.
[10] A. Pagnano, M. Höpf, and R. Teti, "A Roadmap for Automated Power Line Inspection. Maintenance and Repair," *Procedia CIRP*, vol. 12, pp. 234-239, 2013.